UCRL-ID-146496

Resonant Photoemission in f Electron Systems: Pu & Gd

J.G. Tobin, B.W. Chung, R.K. Schulze, J. Terry, J.D. Farr, D.K. Shuh, K. Heinzelman, E. Rotenberg, G.D. Waddill, G. van der Laan

March 7, 2003

U.S. Department of Energy

Lawrence Livermore National Laboratory

DISCLAIMER

This work was performed under the auspices of the U. S. Department of Energy by the University of California, Lawrence Livermore National Laboratory under Contract No. W-7405-Eng-48.

Resonant Photoemission in f electron Systems: Pu &Gd

J.G. Tobin, B.W. Chung,
Lawrence Livermore National Laboratory, Livermore, CA
And
R.K. Schulze, J. Terry, J.D. Farr,
Los Alamos National Laboratory, Los Alamos, NM
And
D.K. Shuh, K. Heinzelman, E. Rotenberg,
Lawrence Berkeley National Laboratory, Berkeley, CA
And
G.D. Waddill,
University of Missouri-Rolla, Rolla, MO
And
G. van der Laan
Daresbury Laboratory, Warrington, WA4 4AD, UK

Abstract

Resonant photoemission in the Pu5f and Pu6p states is compared to that in the Gd4f and Gd5p states. Spectral simulations, based upon and atomic model with angular momentum coupling, are compared to the Gd and Pu results. Additional spectroscopic measurements of Pu, including core level photoemission and x-ray absorption are also presented.

PACS #
71.20 GJ Electronic Str.: Other Metals and Alloys
71.27 +a Strongly Correlated Electron Systems
79.60 -I Photoemission and Photoelectron Spectra

Corresponding Author:
James G. Tobin
LLNL, L-357, POB 808, 7000 East Ave., Livermore, CA, USA 94550
Email: Tobin1@LLNL.Gov; Tel: 925-422-7247; Fax; 925-423-7040

Resonant Photoemission in f electron Systems: Pu &Gd

I. Introduction

While chemically toxic and highly radioactive, Pu may be the most scientifically interesting element in the periodic table. It's properties include the following [1]: six different phases, close to each other in energy and sensitive to variations of temperature, pressure and chemistry; the face-centered-cubic phase (delta) is the *least* dense; Pu expands when it solidifies from the melt; and it is at the boundary between the light (probably metallic) and heavy (probably localized or correlated) actinide elements. Pu remains of immense technological importance and the advancement to a firm, scientific understanding of Pu and its compounds, mixtures, alloys and solutions is a crucial issue. [1, 2] Furthermore, the development of computationally based predictive capabilities hinges upon experimental benchmarking of the variously proposed models. This synchrotron-radiation-based study is the one of the first steps in such an experimental benchmarking. A summary of our resonant photoemission (RESPES) results for Pu is shown in Figure 1. By comparing the Pu 5f and Pu6p results to a RESPES investigation of the 4f system Gd, greater insight will be gained concerning the behavior of 5f electrons and Pu. Finally, the results of an atomic model calculation, for both Gd and Pu , will be presented.

II. Experimental and Computational Details

The experiments were carried out at the SpectroMicroscopy Facility (Beamline 7.0) [3] at the Advanced Light Source in Berkeley, CA, USA. In the photoelectron (x-ray absorption) measurements, the photoelectron (sample

current) intensity was normalized to the photon flux by a Au mesh drain current measured upstream.

Epitaxial Gd (0001) metal films approximately 100 A thick were prepared by e-beam evaporation onto a Y(0001) substrate at room temperature. Details of Gd sample preparation, data collection and a preliminary report of our results can be found in Reference 4 and references therein. The angle resolved photoemission spectra were collected in the chiral geometry using a Perkin Elmer hemispherical energy analyzer with +/-2 degree acceptance angle and with an energy resolution of 250 meV. MLDAD spectra are recorded by reversing the magnetization perpendicular to the plane containing the incident linear light polarization and the detected photoemission, which have a mutual angle of 30 degrees.

The Pu spectroscopy experiments were performed upon three bulk Pu samples, each having a mass of approximately 30mg. Two of the samples were new and highly purified; the third was an aged, weapons grade sample. The new Pu samples were taken from a specially purified batch of Pu metal. [Ref 5 and references therein] The plutonium was zone refined and vacuum distilled while magnetically levitated. The product of the purification process was α-Pu containing a total of 170 ppm impurities. A portion of the refined metal was alloyed with gallium to form the δ-phase (fcc symmetry). The sample surfaces were prepared by repeated room-temperature, sputter-annealing cycles to minimize the amount of oxygen and other impurities dissolved in the sample or at grain boundaries, in a specially designed chamber attached to the sample

introduction and analysis systems on Beamline 7.0. The transfer, preparation, and analysis chambers ensured that the Pu metal samples did not experience pressures greater than 10^{-8} torr. This minimized any surface contaminants that could adversely effect the soft x-ray measurements. Unless other wise specified, the valence band spectra were collected with an energy bandpass of 100meV or better and the wide scans and core level spectra had a bandpass on the order of 350 meV.

For the Gd and Pu , the transition probability for resonant photoemission was calculated using the *t*-matrix approach in first order in the dipole operator and infinite order in the Coulomb decay. These calculations were done in intermediate coupling using Cowan's relativistic Hartree-Fock code. The interference between the direct photoemission channel and the x-ray absorption-Coulomb decay channel was explicitly taken into account by diagonalization of the Hamiltonian for the connected final state. (Only for the Gd5p emission, the interference excluded in order to reduce the overall size of the calculation.)

The Coulomb decay gives rise to a typical decay half-width

$$\Gamma_i = \pi * V^2 \qquad (1)$$

where V is the Coulomb (or super-Coster-Kronig) matrix element, which is proportional to the radial integrals. The interference with the direct photoemission continuum leads to a typical line asymmetry given by a Fano asymmetry parameter,

$$q_i = (D_a)/ (\pi * V * D_e) \qquad (2)$$

where D_a = <5d | r | 5f> is the matrix element for the 5d -> 5f absorption, and D_e = <5f | r | e > is the matrix element for 5f photoemission. (See Figure 2.) If the transition probability for absorption (5d ->5f) is much larger than for direct photoemission (5f ->e), the Fano parameter, q, is large resulting in lineshapes that are rather symmetric. As q approaches infinity, the Fano line shape goes over into a Lorentzian. It is important to note that Γ and q only have a simple meaning for a single line interacting with a continuum. In the presence of multiplet structure, intermediate states of the same symmetry interfere with each other. In this calculation, the interference was explicitly taken into account by diagonalization of the Hamiltonian for the connected final states, $5d^{9}\ 5f^{n+1}$ <-> $5d^{10}\ 5f^{n-1}$ + e. Additional details of the spectral simulations are available elsewhere [4,5,6].

III Pu Sample Quality and Phase Specificity

Considering the significant differences between the new alpha and delta samples versus the aged delta sample, it is useful at this point to perform an elemental analysis using a higher photon energy. Shown in Figure 3 are several wide scans at photon energies of 850eV. The dominant features are all assigned to Pu: 5f (BE = 0eV); 6p (BE = -16 and -29eV); 5d (BE = -102eV); 5p (BE = -210eV) and 4f (BE = -421 and –434 eV). Weaker features can be observed at BE = - 285eV (possibly Carbon 1s (C1s) but actually Pu derived) and BE = -530 eV (Oxygen 1s or O1s). Unfortunately, in the scans with a photon energy of 850eV, the O1s peak is obscured by a larger Pu Auger peak at KE = 310eV. (There is also another Pu Auger peak at KE = 200eV, i.e with a Binding Energy

(BE) near –650 eV at h ν = 850 eV.) Moreover, although the aged delta sample exhibits a significantly different RESPES, the wide scan suggests that all three samples are to a large degree the same in terms of elemental composition, i.e. dominated by Pu features with small O1s peaks. This would seem to rule out one of the proposed explanations for the differences in the aged Pu sample RESPES: surface segregation of the Pu daughter products such as Am. Thus at this point, the remainder of the discussion will focus upon the results for the two new samples, polycrystalline alpha and large crystallite delta. Although very similar in terms of RESPES and wide survey scans, it is possible for the alpha and delta sample to be differentiated.

The issue of sample quality revolves primarily around the level of surface oxidation. Oxygen has three levels : O1s (BE = -529 eV), O2s (BE = - 23 eV), and O2p (BE = - 5 eV). Each level has cross sections which can change dramatically with photon energy, as can the cross sections of the Pu levels. (Below, the cross section calculations of Yeh and Lindau [7] for Oxygen and Plutonium have been utilized. Unfortunately, the calculations of Yeh and Lindau do NOT include the effects of the 5d-5f resonance in Pu.) We will present experimental results which demonstrate the tremendous intensity variations in the regime of the resonance, as well as the Cooper Minimum. To avoid the problem of quantification in this regime, most of the quantitative analysis will be focussed in other more well-behaved photon energy regimes.

IIIa- Phase Differentiation

A number of spectroscopic differences between the alpha and delta phases, particularly with techniques or regimes that favor bulk sensitivity, have been observed. Using total electron yield in x-ray absorption (Figure 4a), a distinct shift between the alpha and delta phases can be discerned. The mean free path for total yield has been estimated to be on the order of 22 angstroms [8], thus this is a fairly bulk sensitive measurement. The shift in Pu is very similar to that reported for α-Ce and γ-Ce phases by Wieliczka et al [9]. Core level photoemission also provides a mechanism for distinguishing the alpha and delta phases. In figure 4b, there are distinct differences between the alpha and delta 4f lineshapes, in agreement with a substantial body of previous work by Naegele [10] and Gouder et al. [11] Again, because of the fairly high kinetic energy of the electrons (about 400 eV), there is a fair amount of bulk sensitivity here. It has been argued in the past [11] that the relative sharpness of the peaks in α-Pu and the large satellite features in δ-Pu are suggestive of delocalization in α-Pu and atomic or electron correlated effects in δ-Pu. Because our samples of Pu are polycrystalline, LEED is not an option.

IIIb- Sample Oxidation Estimation via Pu4f Level Spectra

How do our 4f core level spectra compare to those of known oxides? Pu 4f spectra of PuO2 and other Pu-Oxides are available from the literature and useful to compare to our spectra. Courteix et al [12] provide 4f core level spectra for a series of oxidation levels and using MgKα excitation ($h\nu$ = 1254 eV). (Similar core level spectra can be found in Veal et al [13], for AlKα excitation ($h\nu$ = 1487

eV).) In Courteix et al [12], spectrum a is for nominally clean delta –Pu, spectra b,c and d are for increasing oxidation levels, and spectrum d corresponds to PuO2. It is immediately obvious that the 4f spectra from our delta samples in Figure 4b are qualitatively different than the spectra from the PuO2. (PuO2 has a 4 maximum structure, with separate peaks at BE = -426 eV, -433 eV, -439 eV, and –445 eV.) Thus we can establish the bound that our Pu samples are not remotely similar to PuO2. Courteix et al also conveniently supply O1s spectra, calibrated relative to the Pu4f peaks. We shall return to this later, but looking ahead, we will see that the O1s intensities in our spectra at $h\nu$ = 1250 eV are very much smaller.

IIIc-Oxidation Level Estimation from Valence Band Spectra ($h\nu$=1250eV)

How do our valence band spectra at a photon energy corresponding to a MgK α source (1250 eV) compare to those of known oxides? Again, valence band spectra at $h\nu$ = 1254 eV for Pu-oxides (Courteix et al [12]) and clean Pu (Baptist et al[14]) are available from the literature. Upon examination, it is clear that our spectrum at $h\nu$ = 1250 eV (shown in Figure 5) is very similar to that of Baptist et al and very dis-similar to that of the PuOxides of Courteix et al. Note especially the absence of the O2p and O2s peaks from our spectrum at $h\nu$ = 1250 eV. In the spectra of the PuOxides of Couteix et al at $h\nu$ = 1254 eV [12], there are fairly strong multiple oxygen-derived peaks BE = - 5 eV (O2p), BE = -10 eV (O2p) and BE =- 23 eV (O2s). Again, this is an indication that the oxidation of our samples is fairly limited.

IIId- Quantitative analysis of the O1s intensity

From the hν = 1250 eV spectrum in Figure 6, it is immediately obvious that we have only a very small O1s intensity versus that of the Pu-Oxides of Courteix et al. [12] In our hν = 1250 eV spectrum, the O1s peak can not be seen above the noise. In the PuO2 spectrum of Courteix et al, the O1s peak is approximately 1/3 the height of the Pu 4f peaks. This suggests that we have orders of magnitude less oxygen that the PuO2 sample. To enhance the O1s cross section, we also performed the same measurements at hν = 860 eV. At this photon energy, we can see the O1s (BE = -530 eV) and what may be C1s (BE = -280 eV). By measuring the relative intensities of the O1s and Pu 4f peaks and then correcting for their cross sections (Yeh and Lindau, [7]), we can come up with an O/Pu concentration ratio of 0.06 $\pm$ 0.06 or 6% $\pm$ 6%. The weakness of the O1s feature and uncertainties in the cross section calculations cause the large error bar here.

It should be noted that measurements based upon using the O1s peak are highly preferable to those using the peaks of the O2p and O2s states. This is because (1) the 2p and 2s states are close enough to the valence regime to be affected by changes in bonding and (2) the normalization for the measurements in this regime is usually the valence band or 5f peaks, the intensity of which may also change with chemical state, emission angle, photon energy, kinetic energy etc.

Although in the region labeled as C1s, the peak at BE = -280 eV is actually Pu derived, based upon an analysis of the intensity variations of this

feature and the Pu 4f peaks, using the cross sectional calculations of Yeh and Lindau. Independently, Baptist et al came to a similar conclusion. [14]

Finally, why did we use spectra at 860 eV instead of 850 eV? In our first analysis, we used the spectra at hν = 850 eV. (Figure 3) Unfortunately, at that energy the O1s peak overlaps with a Pu Auger peak, causing the incorrect impression of more oxygen contamination that there actually is. This same Pu Auger peak can also be seen in the hν = 1250 eV spectrum at BE = -950eV. By working at hν = 860 eV, the O1s peak can be isolated from the nearby Auger feature.

IIIe- Photon Energy Dependence of the O2p Peak

Why does the O2p look so big in the spectra at the Cooper Minimum and the 5f anti-resonance? Obviously, we have some oxygen on the Pu samples. By going to where the Pu 5f cross section is very small, it is possible for us to accentuate the Oxygen based features such as the O2p peak at BE = -6eV. Two places where the 5f cross section is the smallest are : (1) the anti-resonance at hν = 102eV and the Cooper Minimum at hν = 220 eV (Figure 7 and Yeh and Lindau, [7]). Looking at the Resonant PES of Pu in Figure 1 and the x-ray absorption in Figure 4, it is easy to see the low intensity of the Pu 5f states at the anti-resonance at hν = 102eV. At the Cooper Minimum, the Pu 5f cross section is about 1/500 of its maximum value. In fact, note the second O2p feature in Figure 7 at BE = -10eV, similar to that observed in the spectrum of PuO_2 at hν = 1254 eV by Courteix et al [12].

The valence band spectra at the Cooper Minimum and the anti-resonance can cause the impression that samples were dirtier than they really were, but this is incorrect. The better analysis is based upon the Pu 4f and O1s peaks, as described above.

IIIf Why are the valence band spectra for the alpha and delta samples so similar? Shouldn't they be more different?

Havela, Gouder, Wastin and Rebizant [11] have shown that a delta like reconstruction forms on alpha Pu if the temperature is room temperature or above. Our gentle annealings (T about 373K) were sufficient to cause the reconstruction on our alpha samples. For this reason, our Pu valence band spectra are qualitatively similar for the two phases, α- Pu and δ- Pu. (E.g. , see Figure 8.) It is worthwhile to note how small O2p peak at BE = -6 eV is at this photon energy. Additionally, it should be mentioned that while the interpretations are significantly different, our observation of spectral similarities for α- Pu and δ- Pu is consistent with the observations of Arko et al [15].

IIIg- Summary result of the Sample Quality Analysis

Although our samples are not quite as clean as those of both Gouder et al [11] and Joyce et al [17], we are in the right regime. Because these are the only known synchrotron -radiation -based PES and X-ray absorption results for Pu and because the sample quality is fairly good, it is worth continuing the analysis.

IV Discussion and Results

IVa- Pu Experiments

Resonant Photoemission in f electron Systems: Pu &Gd

The spectroscopic experiments described here are based upon X-ray Absorption and Photoelectron Spectroscopy (PES). A diagrammatic summary of PES and resonant PES (RESPES) can be found in Figure 2, for the energy levels corresponding to Pu. In a ResPes experiment, the valence band spectrum is collected as the photon energy is ramped through a core level absorption edge. In the case of Pu, the photon energy was scanned through the $O_{4,5}$ (5d) absorption edge. Thus, the result is the 5d5f5f resonant photoemission decay from Pu metal. The final state can be reached by an x-ray absorption - Coulomb decay process, $5d^{10}5f^{n} + h\nu \rightarrow 5d^{9}5f^{n+1} \leftrightarrow 5d^{10}5f^{n-1} + e$, and by direct photoemission, $5d^{10}5f^{n} + h\nu \rightarrow 5d^{10}5f^{n-1} + e$, where e is a photoelectron in a continuum state which has no interaction with the ionic state left behind. Interference between the different pathways results in asymmetric absorption features in the measured spectra. Our Pu studies have been performed with synchrotron radiation as the excitation and are meant to complement earlier Pu studies performed with laboratory sources as the excitation. [11-17].

Photoelectron spectroscopy is a “photon in, electron out” process. Often, it can be simplified down to a single electron phenomenon, where the energy of the photon is absorbed and transferred over entirely to a single electron, while all other “spectator” electrons essentially remain frozen. An advantage of this is its simplicity of interpretation. But in many systems, it is possible to induce a process with heightened sensitivity and significantly increased cross sections: resonant photoemission (ResPes). [4,6,18] Here, a second set of indirect

channels open up, which contribute in concert with the original or direct channel of simple photoemission. Shown in Figure 1 are resonant photoemission results from polycrystalline α-Pu , single crystallite (large grain polycrystalline) δ-Pu and aged polycrystalline δ-Pu. One salient result is that it is abundantly clear that all of the Pu states at and near the Fermi Level have strong 5f character. The overall spectral envelopes are approximately the same, as expected for three samples which are primarily Pu. Nevertheless, significant differences can be observed between the new, purified α and δ samples versus the aged δ-Pu, particularly at the Fermi energy and near a photon energy of 130eV. These results suggest that the valence electronic structure of Pu is dependent upon its phase and chemical state. Nevertheless, overall the three sets of spectra strongly resemble each other and confirm the observation of Pu 5f ResPes.

Resonant Photoemission has a distinct lineshape as a function of photon energy. This can be seen the photoemission results of Figure 1, particularly in the data for the zone refined alpha and delta samples. After an initial pre-resonance regime (near $h\nu$ = 90eV), there is an antiresonance (near $h\nu$ = 100eV) followed by a resonance (maximum near $h\nu$ = 125eV), with an intensity which quickly diminishes as the photon energy increases from 130eV to 150eV. (These results at higher energies are in disagreement with the calculations of Molodstov et al. [19], although the emphasis in their work is upon the behavior near threshold.) Some of this behavior is mimicked in the X-ray absorption measured near the 5d threshold (BE = -102eV), shown in the top panel of Figure 4. Note also, how different the absorption results are for the Pu5d threshold

(near 102eV) versus the Pu4d5/2 threshold (Figure 9, near 800eV). While the RESPES and 5d absorption results for the alpha and delta samples (Figure 1 and 4) exhibit some differences, to a large extent they are quite similar. This can also be seen in the detailed comparison of the Electron Distribution Curves (EDC's), which are plots of photoemission intensity versus electron binding energy for a fixed photon energy. An example of this is shown in Figure 8. A sharp peak near the Fermi energy is followed by a minimum, then a wide peak with a maximum near a binding energy of BE = -1eV. The similarity of the RESPES, EDC's and 5d absorption for alpha and delta Pu is consistent with the recent hypothesis of surface reconstruction of alpha into a delta-like surface [11]. Small additional peaks at BE = - 6eV and – 10eV can be seen, which are attributable to the O2p features of Pu-Oxide, especially PuO2. (These assignments were also discussed in III above.) The high resolution (approximately 100 meV bandpass or better) of the Pu RESPES experiment is confirmed by the sharp Fermi edge jump observed in these spectra.

Another aspect of RESPES in f electron systems is the possibility of a parallel effect in the nearby p state emission. In the case of the Pu 5f RESPES, the related effect would be in the Pu6p states. Figure 10 shows a series of EDC's at photon energies of 100eV (antiresonance), 125eV (resonance), 180eV (off resonance) and 225eV (the 5f Cooper minimum [14]). In the spectra are six major peaks, whose intensities vary distinctly with photon energy. The six are near binding energies of 0eV (Pu5f), -5eV (Oxide O2p), -10eV (PuO2 O2p), -16eV (Pu6p3/2), -23eV (O2s) and –29eV (Pu6p1/2). At resonance (near $h\nu$ =

125eV), the Pu 5f, Pu 6p3/2, and Pu 6p1/2 peaks are strong, overshadowing the smaller O2s and O2p peaks. Off-resonance, at hν = 180eV, the Pu 5f, Pu 6p3/2, and Pu 6p1/2 peaks appear to have similar intensity ratios, but the O2p peaks have increased slightly relative to the Pu features. However, at antiresonance (hν = 100eV) and at the Cooper Minimum (hν = 225eV), O2p peak intensities are substantially increased relative to the Pu5f peak height, near the Fermi energy (BE = 0eV). Interestingly, the 6p:5f ratio appears to be larger at hν = 225eV than at hν = 100eV. This is to be expected, since both the 6p and 5f intensities should be suppressed at the antiresonance (hν = 100eV) but only the 5f (and not the 6p) intensity should be reduced at the the 5f Cooper minimum at hν = 225eV. (The relationship between the O2p and O2s intensities is complicated by the fact that while the O2p cross section is significantly higher at hν < 100eV and both the O2p and O2s cross sections decrease monotonically over the photon energy range of 100 to 300eV, it appears that the O2s and O2p cross section values cross in the vicinity of hν = 200eV. [14] (It should be noted that the calculations of Yeh and Lindau [7] do not include RESPES effects over the photon energy range of 90 to 160eV.)

As mentioned above, the spectra for the new alpha and new delta samples are quite similar. This extends to the EDC's at the Cooper Minimum photon energy of 220eV. As shown in Figure 7, even the Oxygen-Pu ratios are similar.

IVb- Gd Experiment and Theory

At this point it is useful to compare the RESPES of the Pu5f and Pu6p states with that in the Gd 4f and 5p states, respectively. [4] Shown in Figure 11 are photoemission spectra of the Gd 4f states on resonance ($h\nu$ = 150eV) and off resonance ($h\nu$ = 95eV) as well as an x-ray absorption curve for Gd near near the Gd4d thresholds (near BE = - 145eV). One aspect which is immediately obvious when comparing the Gd X-ray absorption near the 4d threshold with the Pu x-ray absorption near the Pu5d threshold is that the Gd has fine structure or pre-peaks below threshold but Pu does not. This is the first of many indicators that the Pu5f states are different from the Gd 4f states. In the case of the Gd 4f and 5p RESPES, one way to get more detailed information is to perform an x-ray magnetic linear dichroism experiment, where the sample is remnantly magnetized first in one direction and then in the reversed direction. (See inset in Figure 11.) [4] Spectra can be collected for each of these configurations: the spectral differences are then a measure of the magnetic dichroism. Shown in Figure 12 are the Gd4f dichroic differences for a series of photon energies. Furthermore, using an atomic model with angular momentum coupling [4,6] it is possible to simulate these differences and their photon energy dependences almost exactly. (See Figure 12.) Similarly, the model works very well for the Gd5p states, as can be seen in Figure 13. Here, the photon energy dependence, fine structure and magnetic dependences exhibited by the experimental results are matched by the theoretical simulations. Again, another manifestation of the more delocalized nature of the Pu states can be seen here. While the Gd 5p

states show a plethora of fine structure, the Pu6p states are smooth and structureless in Figure 10. The Pu results suggest a more metallic or delocalized shielding of the p hole final state, with a washing out of the fine structure associated with the angular momentum coupling which is present in the rare earth elements such as Gd. It also suggests strongly that Pu is non-magnetic, with a small or zero moment per atom.

IVc- Comparison of Pu Experiment to Theory

Now we will compare the experimental results to calculations based upon an atomic model. Theoretically, α-Pu should be more free- electron- like than δ-Pu. Here, we will be looking for trends instead of quantitative agreement. In any case, it is highly useful for us to begin the analysis by comparing our Pu experimental results to an atomic picture of 5f ResPes.

Constant Initial State (CIS) spectra, with fixed binding energy and variable photon energy, are a measure of the absorption and resonant photoemission. (These are slices through the plots in Figure 1 , with fixed binding energies.) Both Pu experimental and calculated atomic results are shown in Figure 14. The calculated 5d absorption spectrum (BE = -12.0 eV) displays a broad structure with roughly three features. The separation into these distinct features is mainly due to the df and ff Coulomb interaction. The two features at lower energy have mainly J = 7/2 and 5/2 character, while the feature at higher energy has mainly J=3/2 character. The line broadening is due to the decay where the Hartree-Fock (HF) value of the half-width Γ is about 3.5 eV. Other decay channels, such 5d5f6s, 5d5f6p, 5d6p6p, and 5d6s6p, were taken into account in the calculation

by including an additional Lorentzian of width Γ_0 = 1 eV. In the calculated spectra, the strong interference between the direct photoemission and the decay makes the absorption structures asymmetric with an intensity minimum around 97 eV due to the Fano anti-resonance. The experimental CIS spectra from δ-Pu show a similar splitting into two peaks with a separation of about 8 eV (117 and 125 eV) and a possible shoulder at lower energy. (In a configuration interaction (CI) model, these satellites can be ascribed to configurations $5d^9 5f^n$. With different n in x-ray absorption [but not in photoemission], the satellite intensities are usually small and a single-configuration approximation is often valid [6] . The reason for this is that after 5d->5f excitation, the 5d core hole is efficiently screened by the additional 5f electron.) The most successful application of the atomic model is its ability to reproduce the relative intensities of the second (Theory 110 eV; Experiment 117 eV) and third peaks (118 eV; 125eV) in the data. The third peak is originally more intense than the second peak. As the binding energy increases (-1.3 eV), the second peak becomes more intense than the third. As the binding energy is further increased the intensities reverses again. This suggests the presence of a remnant of atomic structure in the δ-Pu. This similarity between theory and experiment was not as well observed in the CIS spectra from α-Pu, but still appears to be present. The diminishment of the effect in α-Pu is possibly due to the assumed greater delocalization of the f-electrons in α-Pu sample.

V Summary

High quality ResPes spectra of α-Pu and δ-Pu have been collected and compared to the results of a similar experimental investigation of Gd. Significant agreement has been found to the results of atomic spectral simulations. Nevertheless, it is clear that an atomic model alone will not suffice to explain the observations of 5f Resonant Photoemission in Pu. One salient result is that it is abundantly clear that all of the Pu states at and near the Fermi Level have strong 5f character. Supporting core level measurements and x-ray absorption have been made which confirm the α-Pu and δ-Pu are different. Comparison of Gd5p and Pu 6p results suggest a more metallic, less atomic screening in Pu relative to Gd and also that the Pu has much smaller, if any, magnetic moment per atom. In the future, refined sample preparation and enhanced inclusion of delocalization effects in the theory will be required for further phase specific analyses.

Acknowledgements

This work was performed under the auspices of the U.S Department of Energy by LLNL (Contract No. W-7405-Eng-48), LANL (Contract No. W-7405- ENG-36) and LBNL (Contract No. DE-AC03-76SF00098). The Spectromicroscopy Facility (Beamline 7.0) and the Advanced Light Source were built and are supported by the DOE Office of Basic Energy Research. The authors wish to thank Jason Lashley and Michael Blau for synthesis of the Pu samples. T. Zocco contributed immensely to the Pu experiments at the ALS. D.A. Arena aided in some of the Pu data analysis. F.O. Schumann, S. Mishra and T. Cummins contributed to the Gd data collection and analysis.

References

1. S.S. Hecker, MRS Bulletin **26**, 667 (2001).
2. B.D. Wirth, A.J. Schwartz, M.J. Fluss, M.J. Caturla, M.A. Wall, and W.G. Wolfer, MRS Bulletin **26**, 679 (2001).
3. J.D. Denlinger et al, Rev. Sci. Instrum. **66**, 1342 (1995).
4. S.R. Mishra et al., Phys Rev. Lett. **81**, 1306(1998); J. Vac. Sci. Tech. **A16**, 1348 (1998); J. Vac. Sci. Tech. **A17**, 1313 (1999).
5. J. Terry, R.K. Schulze, J.D. Farr, T. Zocco, K. Heinzelman, E. Rotenberg, D.K. Shuh, G. van der Laan, D.A. Arena, and J.G. Tobin, Surf. Sci. Lett., **499**, L141 (2002); J. Tobin, D.A. Arena, B. Chung, P. Roussel, J. Terry, R.K. Schulze, J.D. Farr, T. Zocco, K. Heinzelman, E. Rotenberg, and D.K. Shuh, J. Nucl. Sci. Tech. **S3**, 98 (2002).
6. G. van der Laan et al. Phys. Rev. B **59**, 8835 (1999); Phys. Rev. B **46**, 9336 (1992); Phys. Rev. B **33**, 4253 (1986).
7. J.J. Yeh and I. Lindau, At. Data Nuc. Data Tables **32**, 1 (1985).
8. P. Bedrossian et al, MRS Proceedings **437**, 79 (1996).
9. D. Wieliczka, J.H. Weaver, D.W. Lynch, and C.G. Olson, Phys. Rev **B26**, 7056 (1982).
10. J.R. Naegele, J. Nucl. Matl. **166**, 59 (1989); Chapter 2.8 of "Electronic Structure of Solids: Photoemission Spectra and Related Data," ed. A. Goldmann and E. Koch, Landolt-Bornstein Numerical Data and Functional Relationships in Science and Technology, Group III, Vol. 23, Springer-Verlag, Berlin, Germany, 1994.
11. T. Gouder, Europhys. Lett. **55**, 705 (2001); MRS Bulletin **26**, 684 (2001); Phys. Rev. Lett. **84**, 3378 (2000); J. Alloys Cmpds. **271-273**, 841 (1998); J. El. Spect. Rel. Phen. **101-105**, 419 (2000); L. Havela, T. Gouder, F. Wastin, and J. Rebizant, Phys. Rev. **B65**, 235118 (2002).
12. D. Courteix et al, Solid State Commun. **39**, 209 (1981).
13. B.W. Veal et al, Phys. Rev. **B15**, 2929 (1977).
14. R. Baptist et al., J. Phys. F (Metal Phys.) **12**, 2103 (1982).
15. A.J. Arko, J.J. Joyce, L. Morales, J. Wills, J. Lashley, F. Wastin, and J. Rebizant, Phys. Rev. **B 62**, 1773 (2000); A.J. Arko etal.,J. Alloys Cmpds **271-273**, 826 (1998) and **286**, 14 (1999).
16. J. Joyce, private communication and Bulletin APS **47**, 960 (2002).
17. L.E. Cox et al, Phys. Rev. B **46**, 13571 (1992); Phys. Rev. B **37**, 8480 (1988).
18. K. Starke et al.,Phys. Rev. B **55**, 2672 (1997).
19. Molodstov et al, Phys. Rev. Lett. **87**, 017601 (2001).

Resonant Photoemission in f electron Systems: Pu &Gd

Figure Captions

Figure 1: Resonant Photoemission (ResPes) data sets are shown here, for a polycrystalline α (top), single crystallite δ (middle) , and aged polycrystalline δ (bottom.) The plots show the intensity variations (z axis) versus the binding energy of the states (the negative numbers in eV; zero is the Fermi energy) and photon energy (between 90eV and 160eV). The alpha sample has been zone refined and is polycrystalline. The delta sample has been prepared by doping the alpha sample material with Ga and is large crystallite. The aged sample is delta and polycrystalline. These results suggest that RESPES is directly sensitive to changes in valence electronic structure associated with structural and chemical variations. The bandpass was 100meV or less throughout.

Figure 2: Schematic of the resonant photoemission process. Photoemission is a “photon in- electron out” process. In conventional Photoelectron Spectroscopy, a single electron/ single channel is involved.
In RESPES, additional indirect channels with multiple electrons can participate, increasing the cross section and sensitivity of the process.

Figure 3: Pu wide photoemission scans at 850 eV, for a polycrystalline α- Pu (top), single crystallite δ- Pu (middle) , and aged polycrystalline δ- Pu (bottom). The bandpass was about 350 meV in these spectra.

Figure 4(a): X-ray absorption of Pu at the 5d threshold ($O_{4,5}$), from a large crystallite δ-Pu sample and a polycrystalline α-Pu sample. The instrumental bandpass was 40 meV or better throughout.

Figure 4(b): Core-level photoemission spectra from a large crystallite δ-Pu sample and a polycrystalline α-Pu sample are shown. These spectra were collected with a photon energy of 850 eV and a bandpass of about 350 meV.

Note that two large components are visible in each spectral structure, a sharp feature at low binding energy and a broad feature at higher binding energy.

Figure 5: PES Spectrum of α- Pu at $h\nu$ = 1250 eV. Note the presence of the features associated with the Pu 5f (BE = 0 eV), Pu 6p3/2 (BE = -16 eV), and Pu 6p1/2 (BE = -29 eV) but the absence of oxygen derived features, e.g. the O2p (BE = -5 eV, -10 eV) and O2s (BE = -23 eV). The effective resolution here is degraded below that of the 200- 300 meV bandpass quoted for the other Pu spectra, being on the order of 0.6 eV.

Figure 6: Wide scans of δ-Pu at photon energies of 860eV (bandpass of 0.35 eV) and 1250eV (bandpass of about 0.6 eV) are shown here. The oxygen (O1s, binding energy of -530 eV) is much more easily observed at 860eV (black curves) than at 1250eV (red curves). The inset shows an enlargement of that region for each photon energy.

Figure 7: Photoemission EDC's near the Cooper Minimum of the Pu 5f states are shown here, for both the large crystallite δ-Pu sample ($h\nu$ = 220 eV) and the polycrystalline α-Pu sample ($h\nu$ = 225 eV). Here at the Cooper minimum, the Pu5f intensity is diminished and the oxygen peaks at –5eV and –10eV are relatively enhanced. The instrumental bandpass was 0.1 eV or lower for both of these spectra.

Figure 8: EDC's of large crystallite δ-Pu sample and a polycrystalline α-Pu sample at a photon energy of 125eV are shown. Note the sharp rise at the Fermi edge, indicative of the 100meV bandpass. The bandpass contribution (100 meV or less) and the thermal contribution (about 0.113eV at Room Temperature) combine to give a width at the Fermi Edge (BE = 0 eV) of about 0.2 eV.

Figure 9: X-ray absorption spectrum of α-Pu at the 4d ($N_{4,5}$) threshold. Only the Pu 4d 5/2 peak is shown. The bandpass was 0.4 eV or better throughout.

Figure 10: EDC's of alpha Pu at photon energies of 100eV (antiresonance, bottommost), 125eV (on resonance, 2nd from bottom), 180eV (off resonance, 2nd from top), and 225eV (Cooper minimum, topmost). The experimental bandpass was 100 meV or better throughout.

Figure 11: The x-ray absorption and photoemission of Gd thin films. In the upper panel is x-ray absorption near the 4d threshold, showing the pre-peak structure at 137eV and 142eV and the giant resonance at 148eV. Below is 4f photoemission, both on (150eV) and off (95eV) resonance. The inset shows the experimental geometry.

Figure 12: A series of experimental and theoretical Gd 4f photoemission dichroism spectral difference curves. On the left are the experimental curves, on the right are the theory curves. From the top, the photon energies are 95eV, 142eV, 146eV and 150eV. PND stands for peak normalized difference, where the dichroism difference at each binding energy is divided by the sum of the two intensity maxima, one from each spectral pair. (Not shown, Following Ref. 4.) The photon energy of 150 eV is "on" resonance and 95eV is "off" resonance.

Figure 13. A series of experimental and theoretical Gd 5p photoemission spectra (for the two opposite magnetization directions). (a) $h\nu$ =137 eV, experimental. (b) $h\nu$ =140 eV, experimental. (c) $h\nu$ =142 eV, experimental. (d) $h\nu$ = 149.6 eV, experimental.(e) $h\nu$ =151 eV, experimental. (f) $h\nu$ =137eV, theory. (g) $h\nu$ = 140eV, theory. (h) $h\nu$ =142 eV, theory. (i) $h\nu$ =149.6 eV, theory. (j) $h\nu$ = 151 eV, theory. EDC is energy distribution curve. The experimental spectra are EDC's, where the photon energy is held constant and the kinetic energy is scanned. The relative intensities of the experimental curves were determined by

normalizing to the valence band intensities and then correcting for the valence band cross sections. (See Ref. 4)

Figure 14: The constant initial state spectra (CIS) are shown: (a) α-Pu; (b) δ-Pu; and (c) atomic theory . (a)The calculated spectra are shown at the binding energies of 0.0, -0.5, -1.3, -2.1, -3.2, and -12.0 eV. The experimental spectra are shown at similar binding energies. Note that in both the calculated and measured δ-Pu spectra, the intensity of the second and third peaks switch as the binding energy increased.

Resonant Photoemission in f electron Systems: Pu &Gd

Figure 1

(a) α-Pu

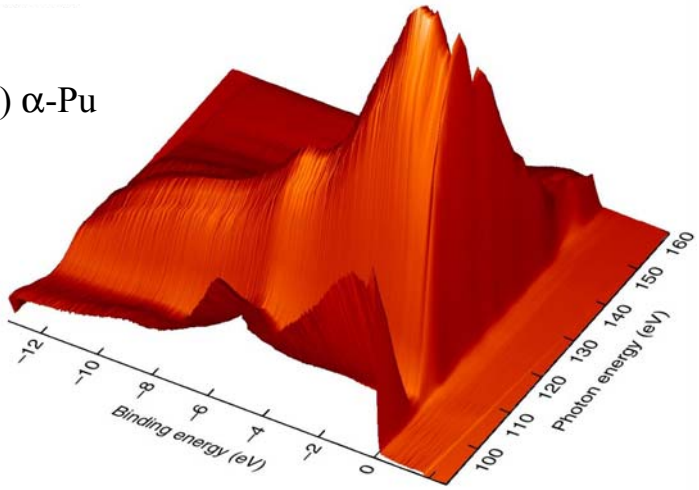

(b) δ-Pu

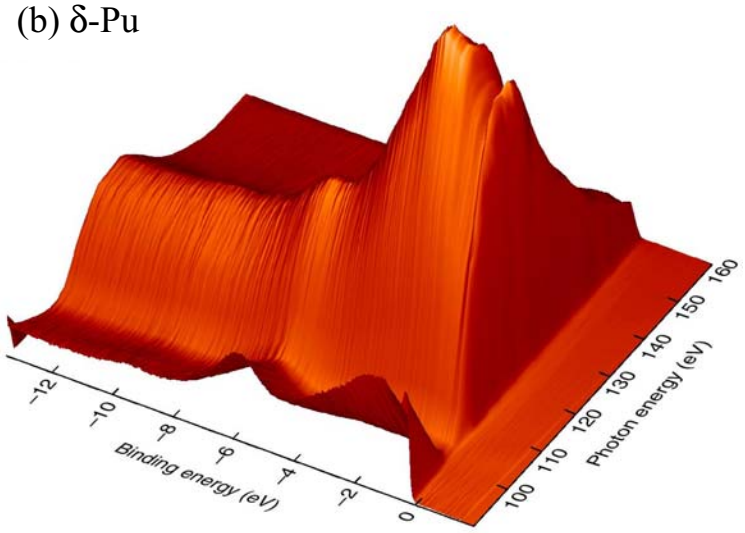

(c) aged-Pu

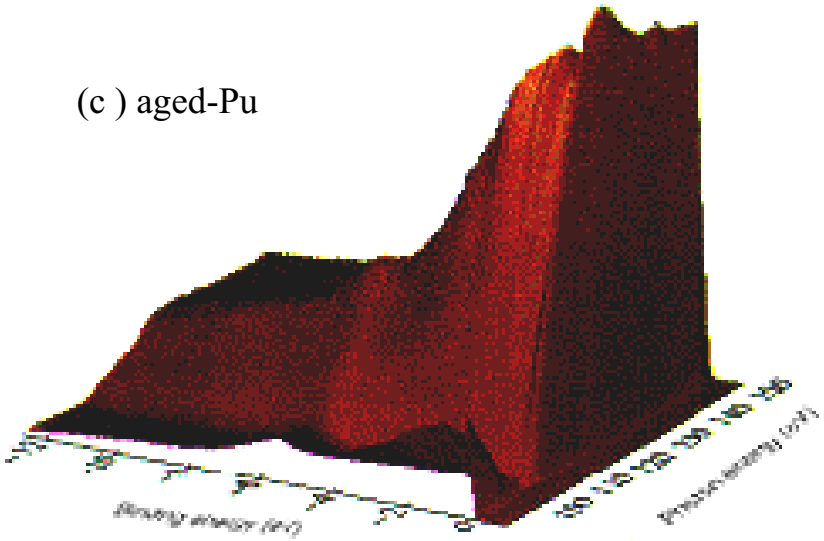

Resonant Photoemission in f electron Systems: Pu &Gd

Figure 2

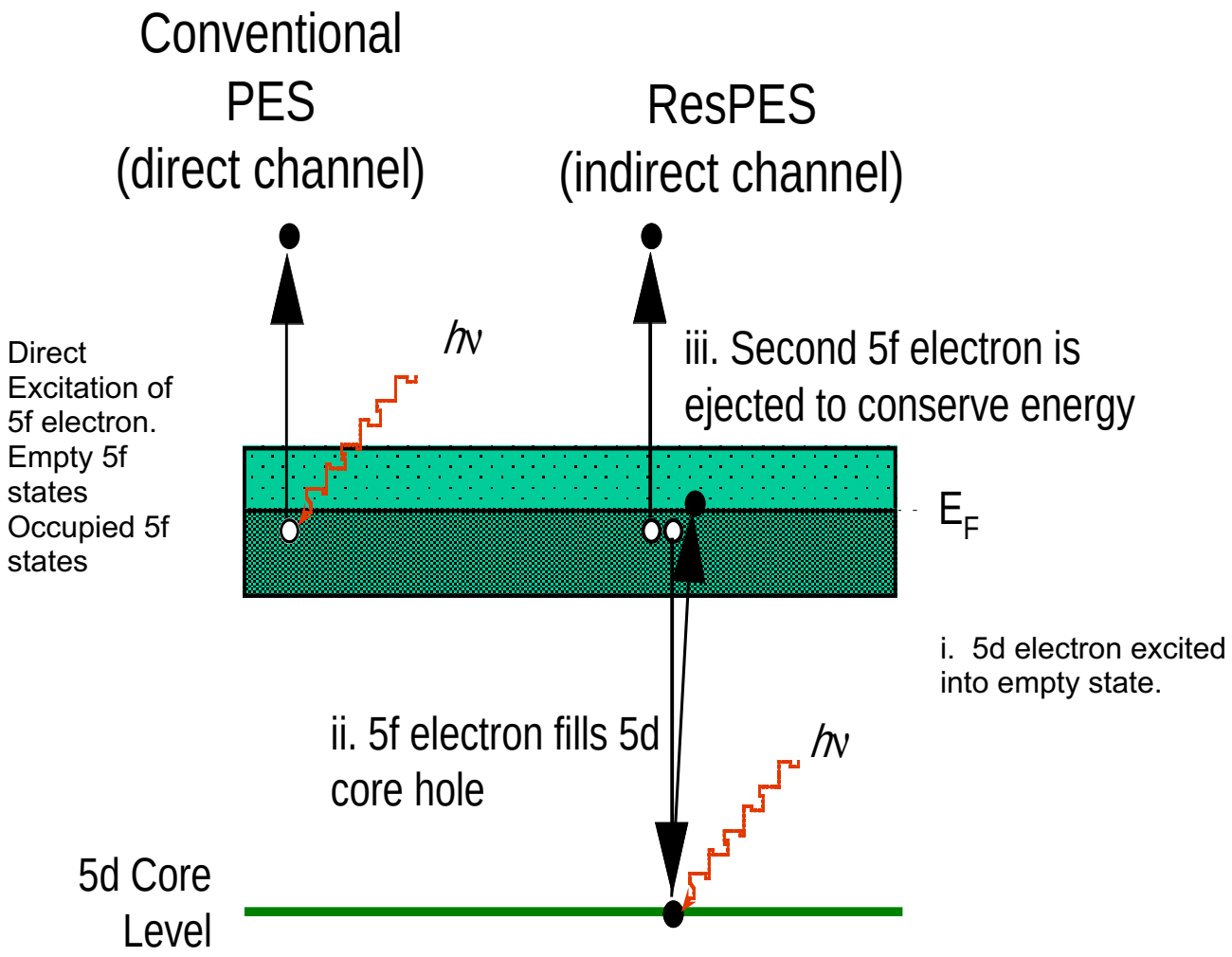

Resonant Photoemission in f electron Systems: Pu &Gd

Figure 3

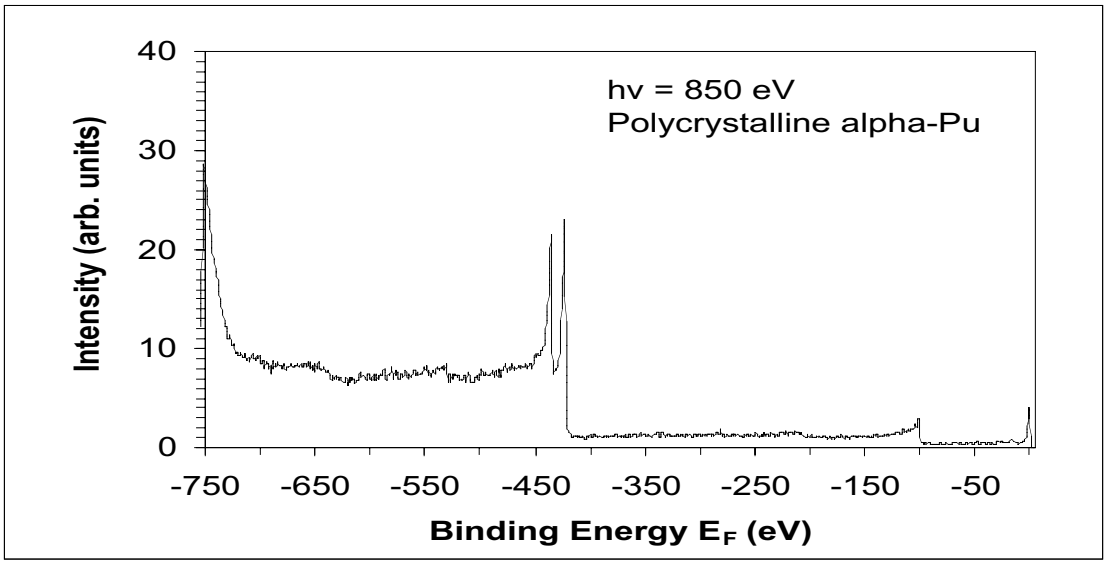

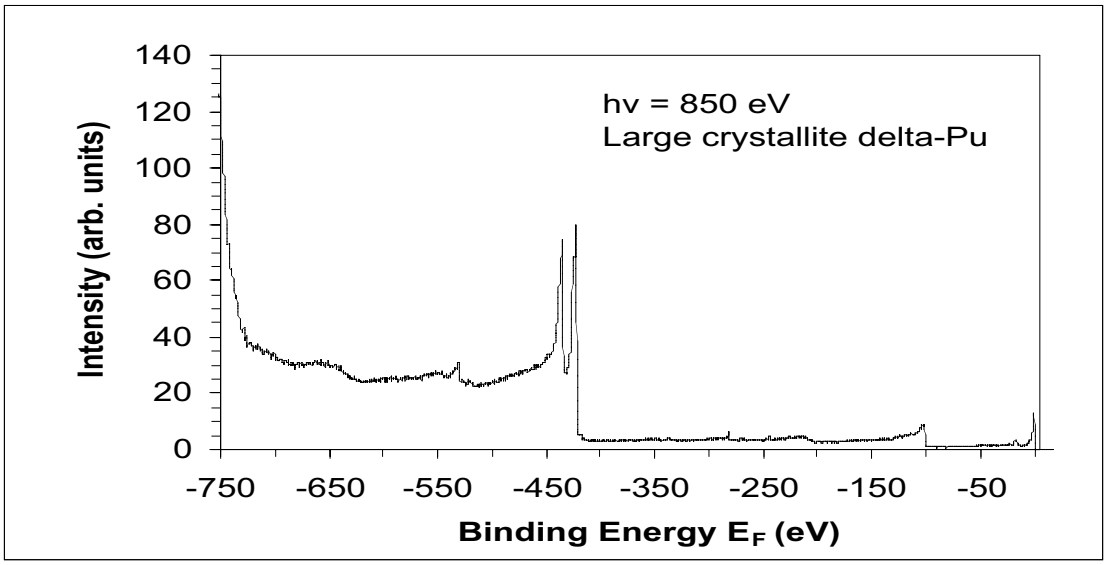

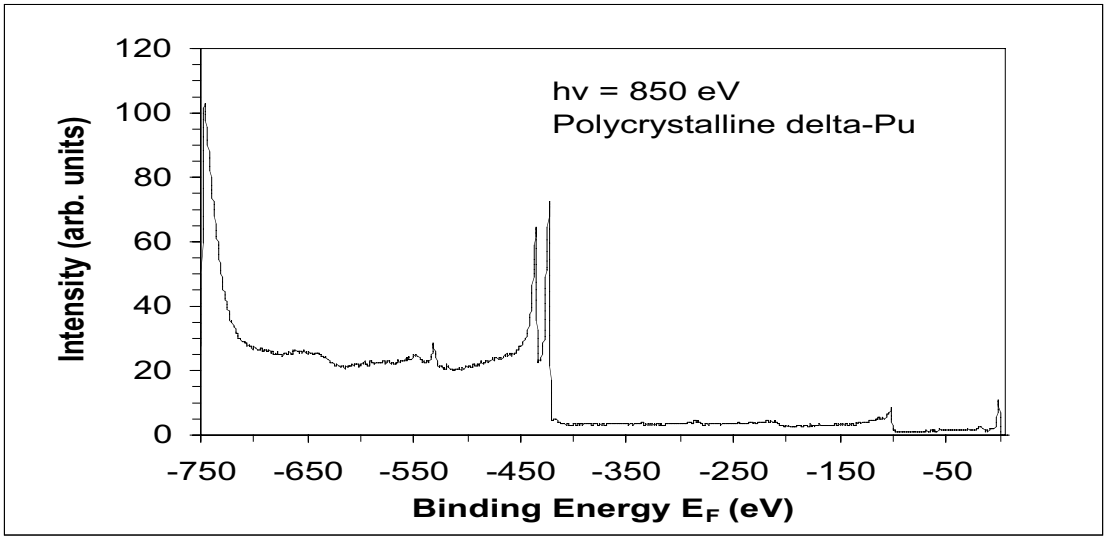

Figure 4

Figure 4a

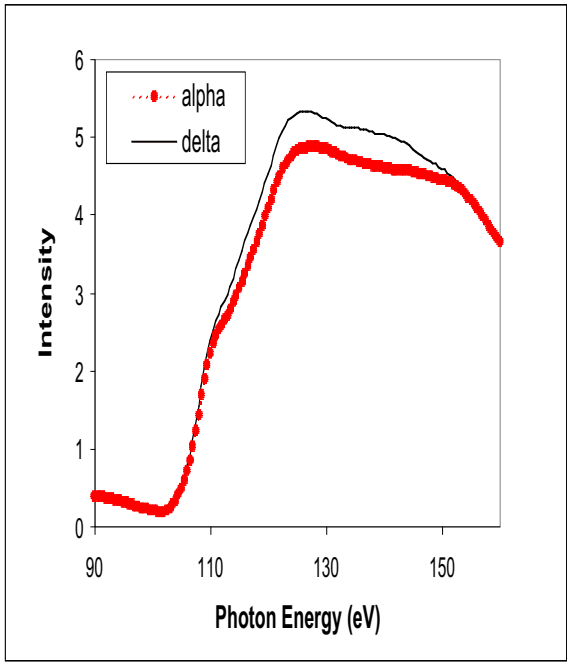

Figure 4b

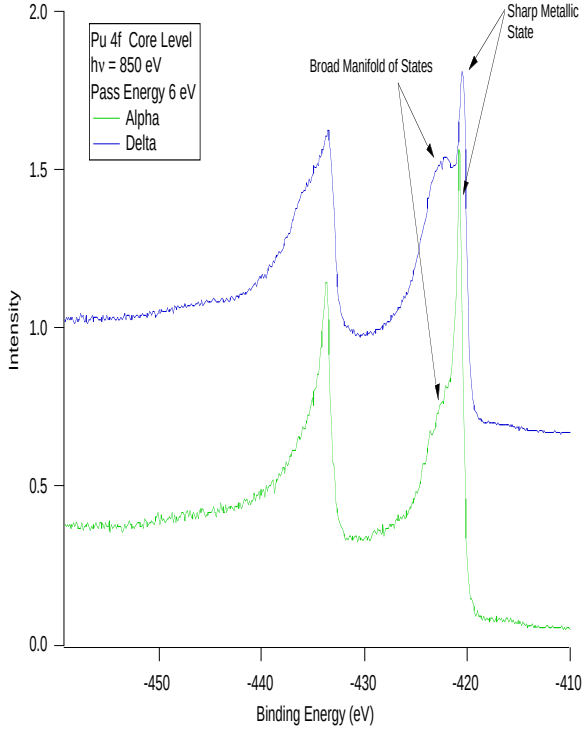

Figure 5

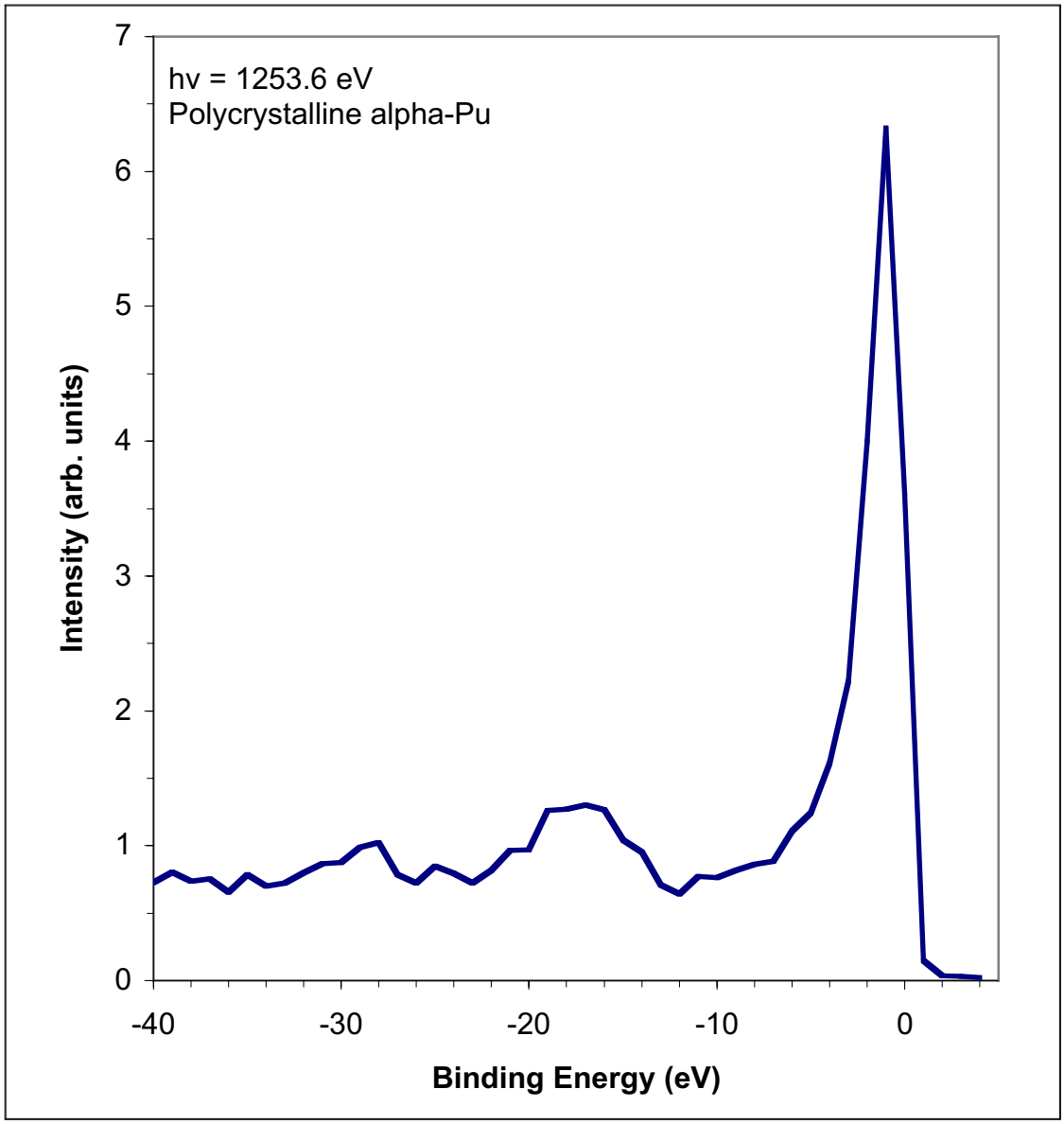
hv = 1253.6 eV
Polycrystalline alpha-Pu
Intensity (arb. units)
Binding Energy (eV)
0
1
2
3
4
5
6
7
-40
-30
-20
-10
0

Resonant Photoemission in f electron Systems: Pu &Gd

Figure 6

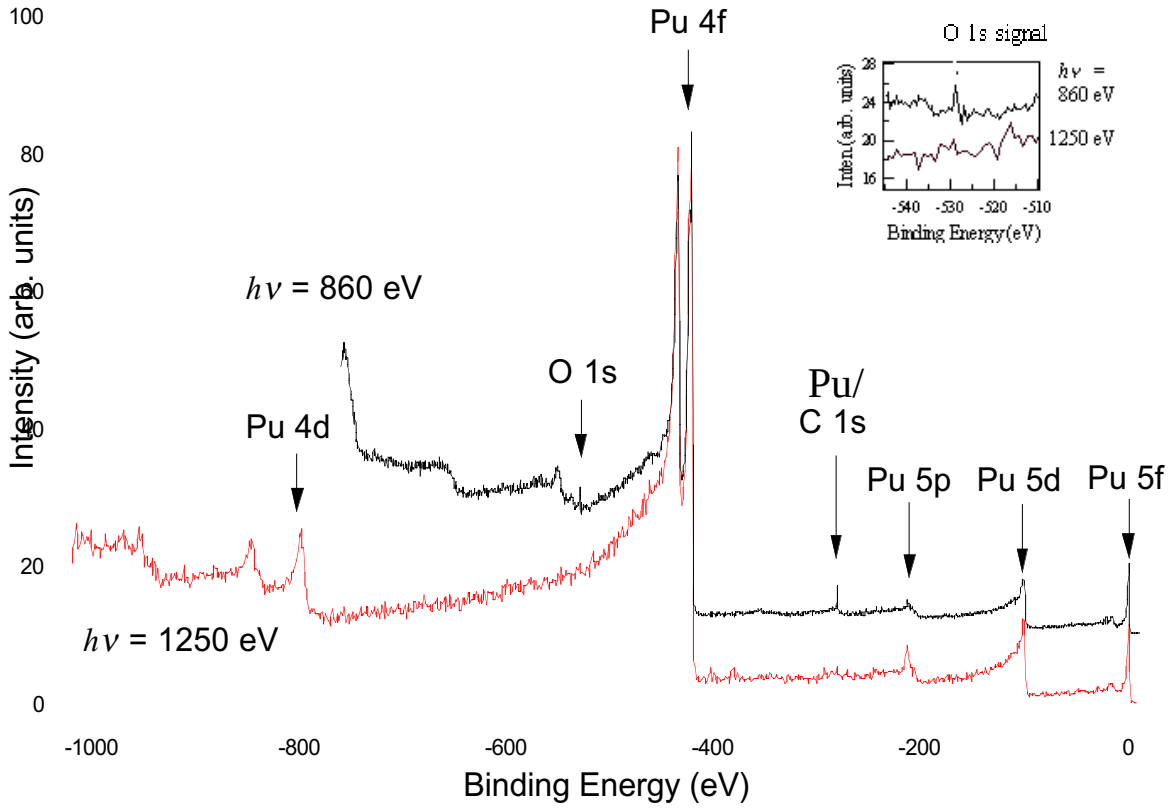

Figure 7

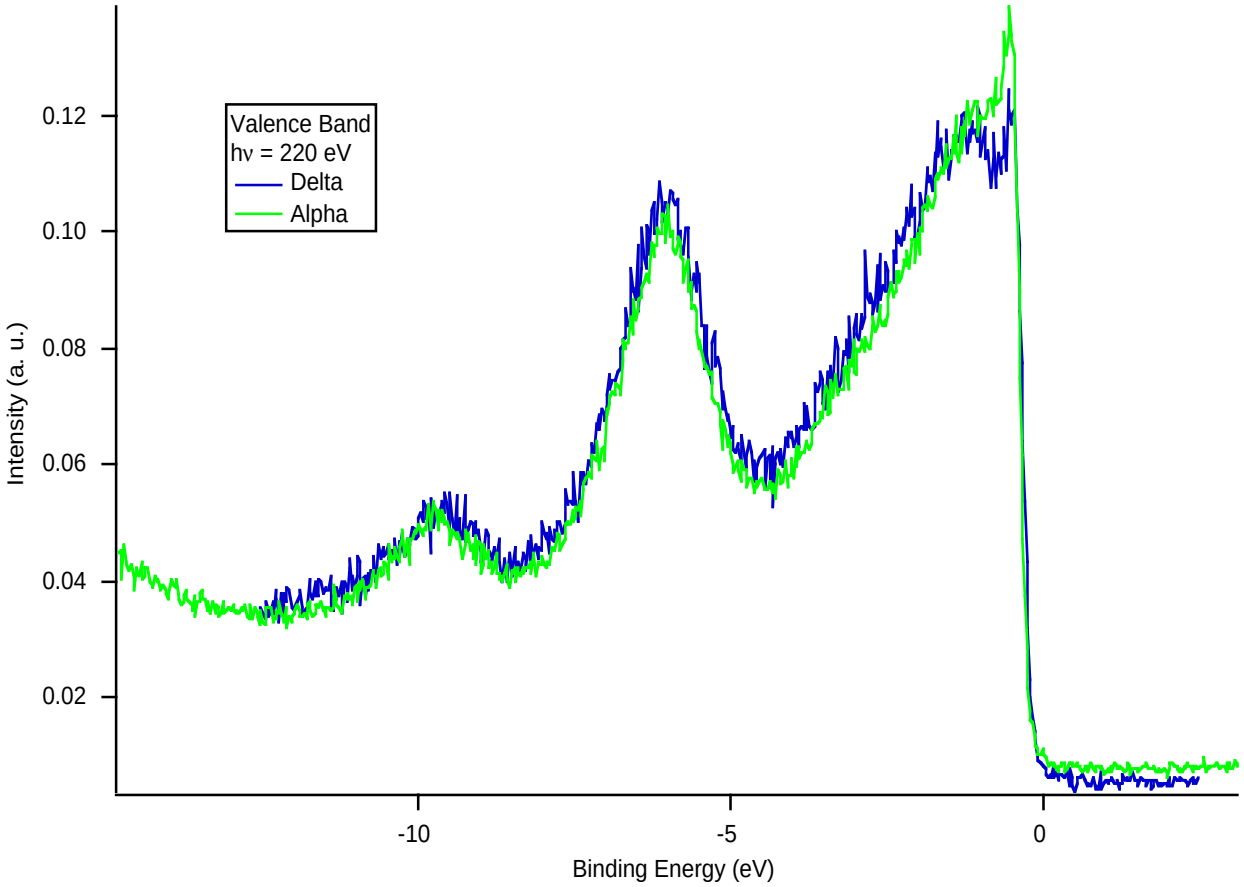
Valence Band
hν = 220 eV
Delta
Alpha
Intensity (a. u.)
0.12
0.10
0.08
0.06
0.04
0.02
-10
-5
0
Binding Energy (eV)

Resonant Photoemission in f electron Systems: Pu &Gd

Figure 8

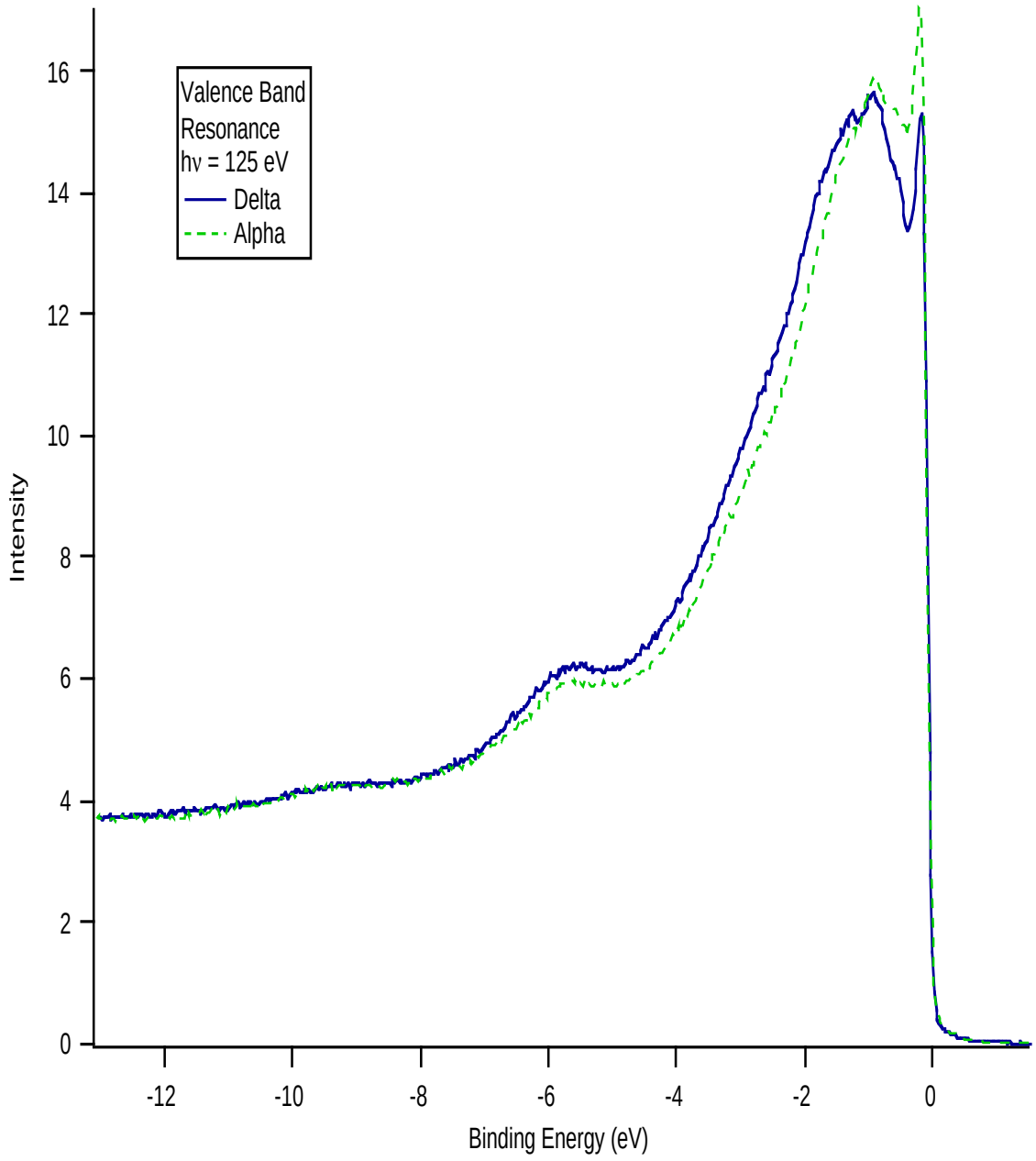

Figure 9

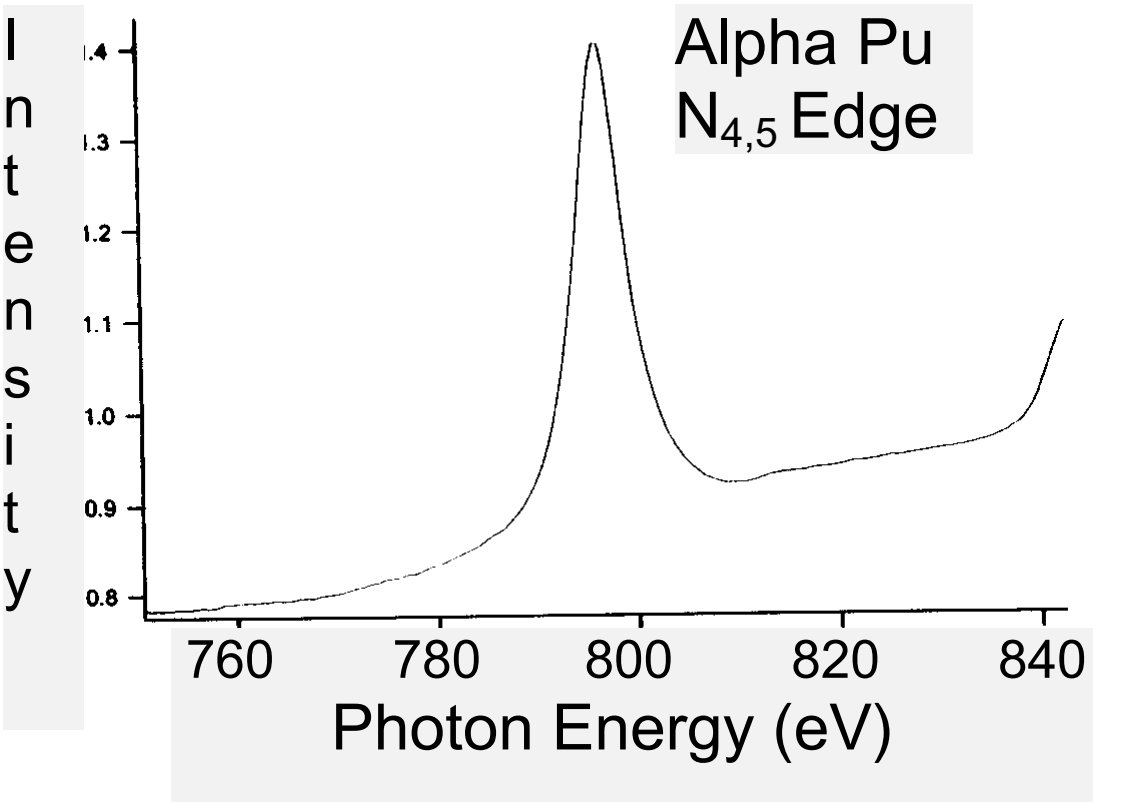
Intensity
1.4
1.3
1.2
1.1
1.0
0.9
0.8
Alpha Pu
$N_{4,5}$ Edge
760
780
800
820
840
Photon Energy (eV)

Resonant Photoemission in f electron Systems: Pu &Gd

Figure 10

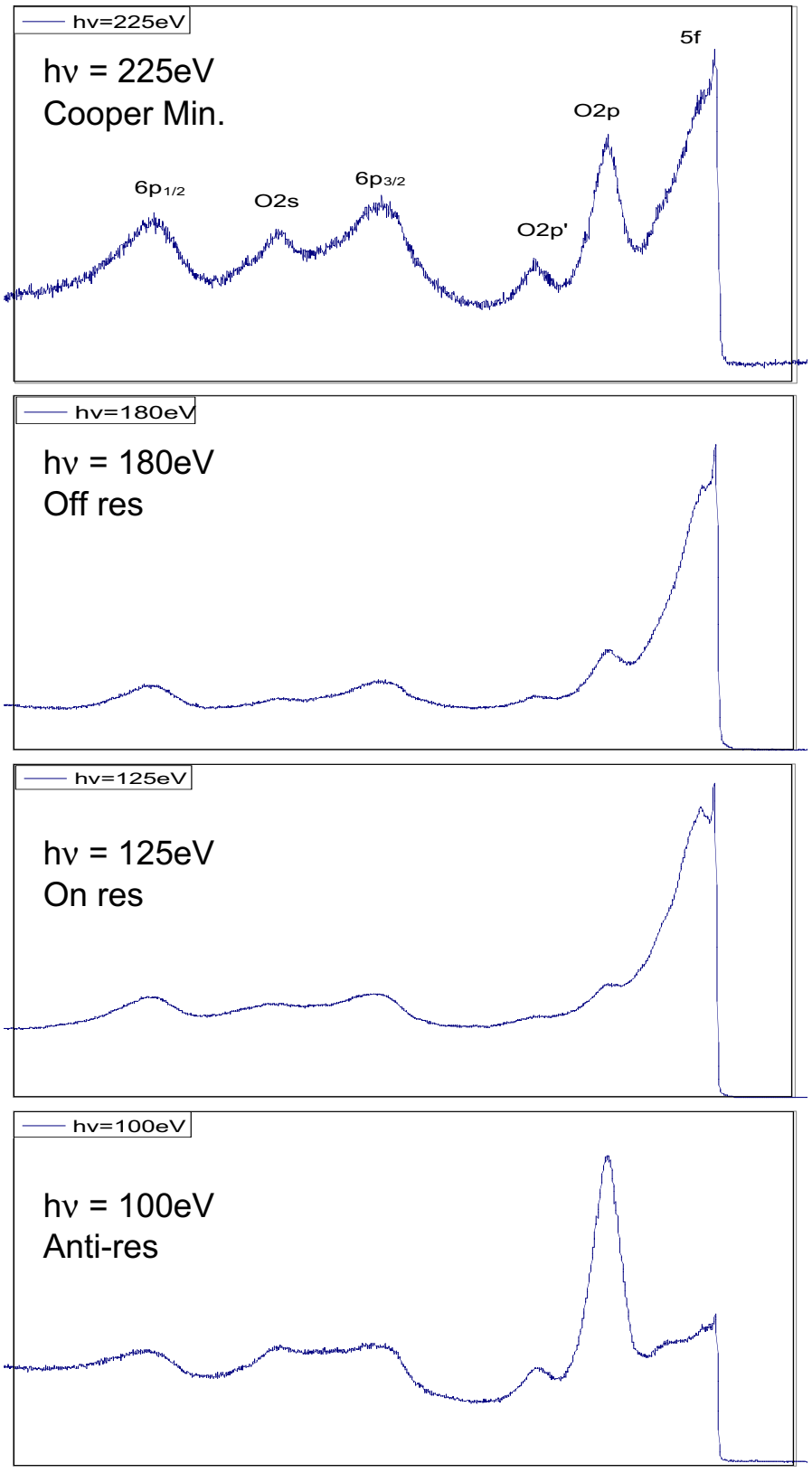

Resonant Photoemission in f electron Systems: Pu &Gd

Figure 11

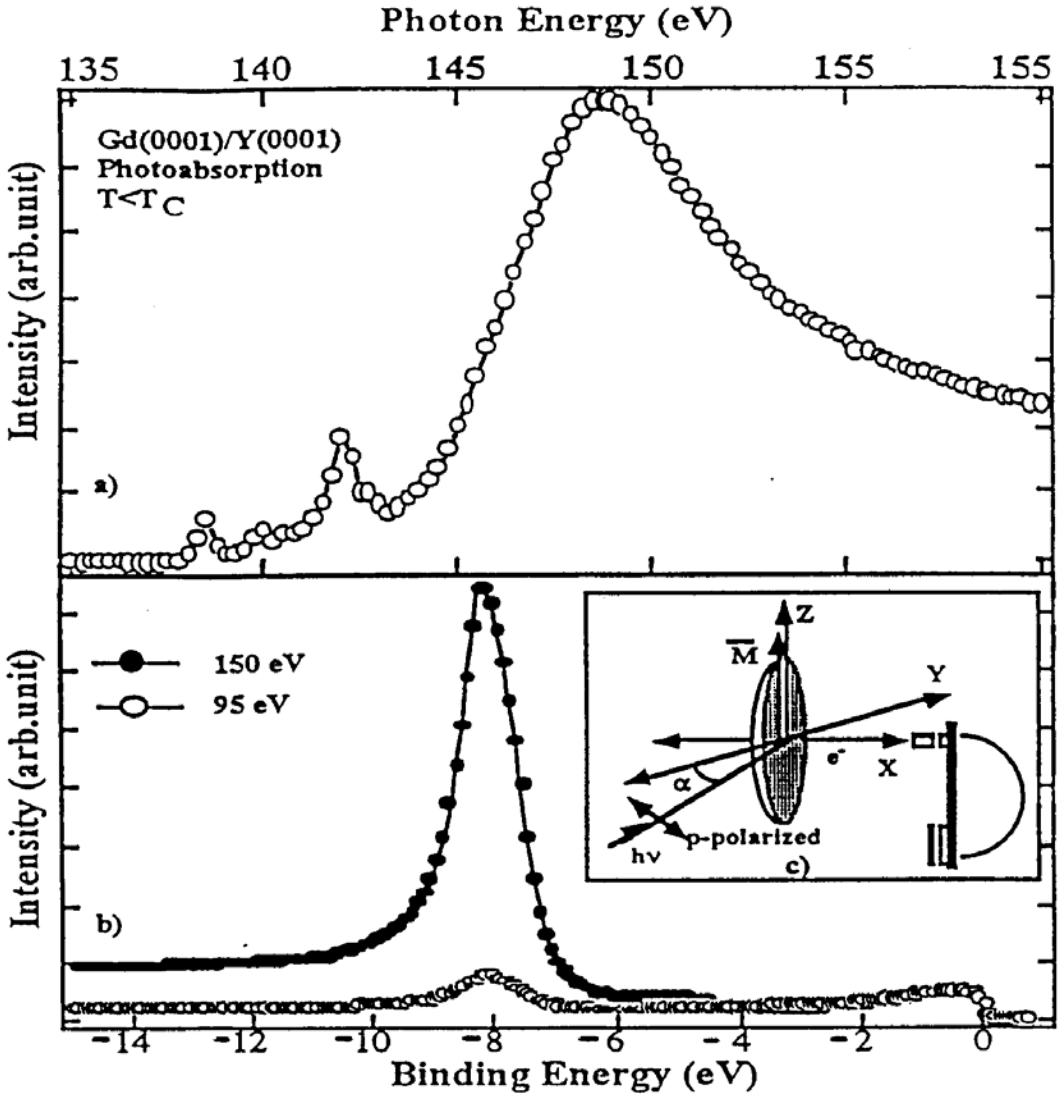

Figure 12

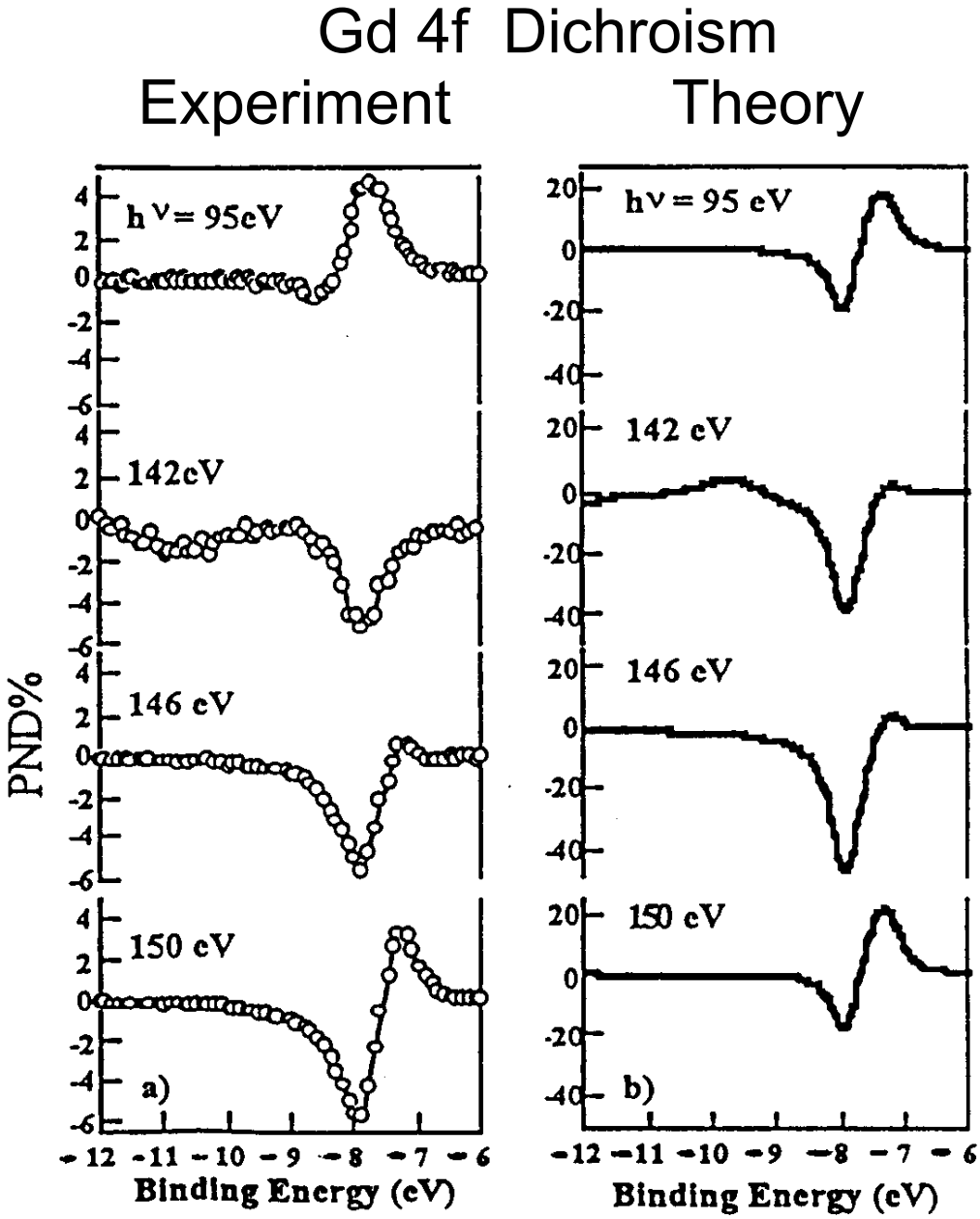
Gd 4f Dichroism
Experiment
Theory
hν = 95eV
142eV
146 eV
150 eV
PND%
a)
b)
Binding Energy (eV)
Binding Energy (eV)

Figure 13

Gd 5p Dichroic Spectra

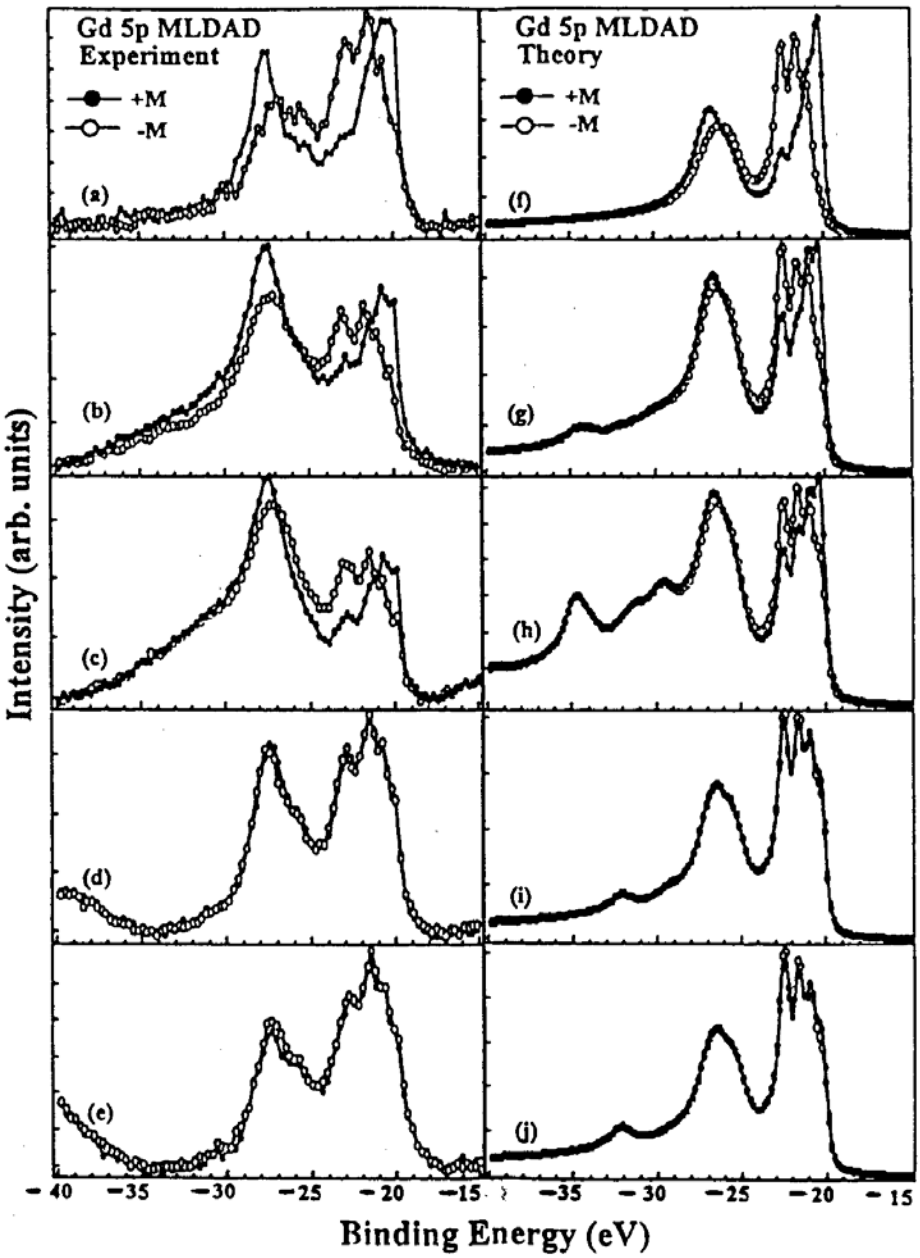

Resonant Photoemission in f electron Systems: Pu &Gd

Figure 14

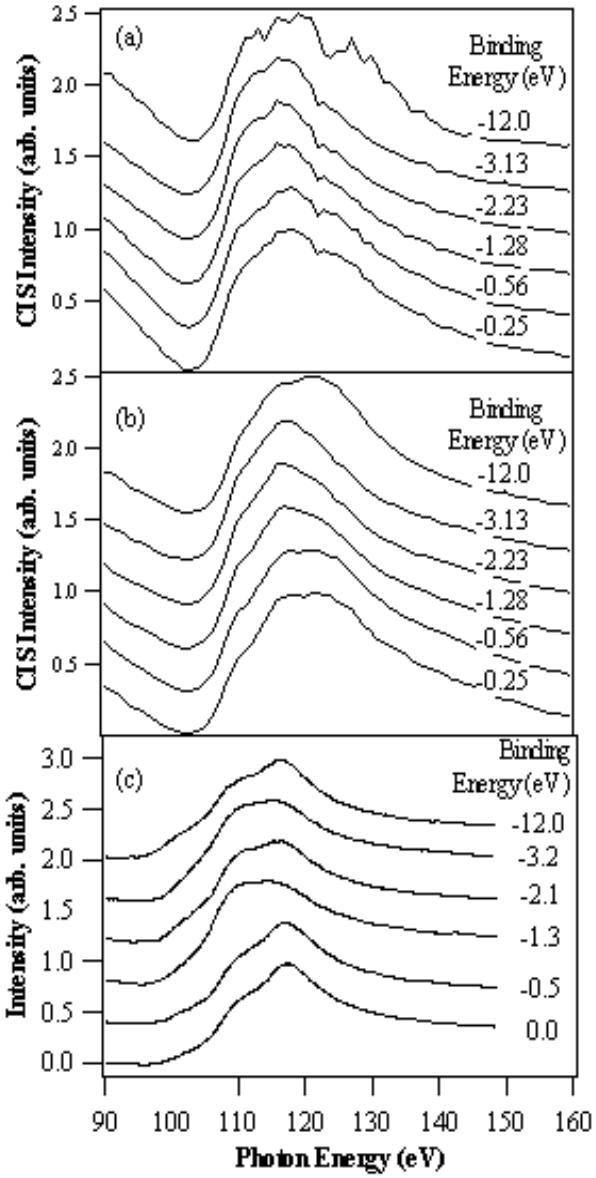

(a) CIS Plots for polycrystalline α-Pu
(b) CIS Plots for large crystallite δ-Pu
(c) Theoretical CIS plots for atomic Pu